Understanding the setting and hardening process of wollastonite-based brushite cement. Part 1: Influence of the Ca/P ratio and H3PO4 concentration of the mixing solution

Priscillia Laniesse, Céline Cau Dit Coumes, Gwenn Le Saout, Adel Mesbah

Understanding the setting and hardening process of wollastonite-based brushite cement. Part 1: influence of the Ca/P ratio and H_3PO_4 concentration of the mixing solution

Priscillia Laniesse[a*], Céline Cau Dit Coumes[a], Gwenn Le Saout[b], Adel Mesbah[c]

[a] CEA, DES, ISEC, DE2D, Univ Montpellier, Marcoule, France

[b] IMT Mines Alès, C2MA, 30319 Alès, France

[c] Institut de Chimie Séparative de Marcoule, ICSM, CEA, CNRS, ENSCM, Univ Montpellier, Marcoule, France

* Corresponding author

Tel.: +33 6 19 14 68 97

e-mail address: priscillia.laniesse@insa-toulouse.fr

Abstract (≤ 150 words)

Wollastonite-based brushite cement are prepared by mixing wollastonite with a phosphoric acid solution containing metallic cations and boric acid. This work investigates simplified systems comprising wollastonite and H_3PO_4 solutions only, in order to clarify the influence of the H_3PO_4 concentration, Ca/P and l/s ratios (this latter parameter being correlated to the two others) on the setting and hardening process.

At constant H_3PO_4 concentration, increasing the Ca/P ratio, and decreasing the l/s ratio, accelerates the early stages of hydration but limits its progress at 7 d. At high Ca/P ratio, more basic calcium orthophosphates form in addition to dicalcium phosphate.

At constant l/s ratio, increasing the H_3PO_4 concentration in the range 7-10 $mol.L^{-1}$ retards cement hydration, and inhibits the setting at concentrations ≥ 12 $mol.L^{-1}$. A good compromise is obtained for H_3PO_4 concentrations between 9 and 10 $mol.L^{-1}$: hydration is not too fast and yields the maximum amount of dicalcium phosphate.

Keywords: hydration (A), hydration products (B), chemically bonded ceramics (D), Thermodynamic calculations (B)

1. Introduction

Phosphate binders are often referred as “chemically bonded phosphate ceramics” because they can produce materials with low porosity and high mechanical strength [1, 2]. However, their setting and hardening process results from a dissolution / precipitation process, yielding to crystallized hydrates of low solubility, often associated with poorly characterized amorphous phases. This work is focused on brushite cements prepared from wollastonite ($CaSiO_3$), a natural calcium meta-silicate, and phosphoric acid (H_3PO_4) mixing solution, as firstly described by Semler [3, 4]. These binders can exhibit very good thermal resistance after hydrothermal post-treatment and are thus mainly used for refractory applications [5, 6]. They are also of interest for sealing and bonding due to their good adhesion properties with wood, ceramics and concrete [7]. Their potential for radioactive waste management has been pointed out more recently. Composite materials incorporating up to 50% of lead oxide by weight of cement may be used for radiation shielding [8]. Besides, Laniesse *et al.* [*9*] have shown that wollastonite-based brushite cements may show a better chemical compatibility with acidic radwaste than conventional calcium silicate cements and can improve the confinement of strontium [10].

In contrast with Portland cement, the setting and hardening process occurs under acidic conditions [5]: the reaction starts in very acidic medium (pH < 1), but the pH increases rapidly to reach an equilibrium which depends on the Ca/P ratio of the material. Mosselmans *et al.* [11] investigated model systems comprising wollastonite and a 13 mol% phosphoric acid (corresponding to a concentration close to 3.8 mol/L) with Ca/P molar ratios varying between 0.34 and 2.56. At Ca/P ratios higher than 1, brushite and amorphous silica were the two main products formed according to mass balance equation (Eq. 1):

$$CaSiO_3 + H_3PO_4 + (1+x)\,H_2O \rightarrow SiO_2.xH_2O + CaHPO_4.2H_2O \qquad \text{(Eq. 1)}$$

At lower Ca/P ratios (between 1 and 0.34), monetite ($CaHPO_4$) and calcium dihydrogenophosphate monohydrate ($Ca(H_2PO_4)_2.H_2O$ –MCPM) additionally precipitated. When the Ca/P ratio is less than 0.71, brushite was not observed anymore.

In practice, wollastonite-based binders are prepared with more concentrated phosphoric acid solutions (typical concentrations of 9-10 $mol.L^{-1}$). To avoid flash setting as well as excessive heat output, retarders, such as boric acid or borax, are added, as well as metallic cations (typically Al^{3+}, Zn^{2+}, Mg^{2+}) [3, 6, 12, 13]. A recent paper [14] reports a thorough investigation of the hydration of a commercial binder prepared by mixing wollastonite with a phosphoric acid solution ($[P]_{tot}$ = 9.3 $mol.L^{-1}$) comprising Al^{3+} and Zn^{2+} cations (at concentrations of 1.3 $mol.L^{-1}$) and borax ($[Na_2B_4O_7]$ = 0.15 $mol.L^{-1}$) at a liquid/solid ratio of 1.25 (resulting in a molar Ca/P ratio of 1.2). A multi-step process was evidenced:

- monocalcium phosphate monohydrate (MCPM - $Ca(H_2PO_4)_2.H_2O$) formed transiently,
- an amorphous phase containing Al, Zn and Ca massively precipitated during the first minutes after mixing, and progressively became richer in calcium as hydration progressed,
- brushite ($Ca(HPO_4).2H_2O$) formed once MCPM started to destabilize.

There is however a lack of data about the influence of a variation in the composition of the mixing solution on the cement hydration process and properties of the resulting material. In this work, the focus is placed on the effect of the phosphoric acid concentration, Ca/P molar ratio and liquid-to-solid (l/s) weight ratio, with investigated domains relevant for wollastonite-based brushite cement pastes. A second paper will be more specifically dedicated to the role of metallic cations.

2. Experimental

2.1 Materials and specimen preparation

The wollastonite powder was provided by Sulitec. It also contained small amounts of calcite and quartz which were evidenced by X-ray diffraction and thermogravimetric analysis (TGA and XRD diagrams are given in [14]). The proportion of calcite was assessed to be 1.6 ± 0.1 wt.% (weight loss due to $CaCO_3$ decarbonation recorded by TGA at 654°C). The particle size distribution of the powder, determined by laser granulometry, ranged between 0.5 µm and 135 µm (d_{10} = 2.8 µm, d_{50} = 15.2 µm, d_{90} = 48.3 µm). The wollastonite particles had a needle shape. Their mean aspect ratio (ratio of the length-to-diameter), which was determined using SEM images of c.a. 100 particles, was close to 4:1.

The mixing solution was a phosphoric acid solution, prepared from a 85%wt. H_3PO_4 (14.6 $mol.L^{-1}$) analytical grade commercial solution provided by VWR. As the solution was initially very acidic, its pH could not be measured directly with a pH electrode. Therefore, its acidity function H_0 was determined. This function was first developed by Hammett [15] and provides a quantitative measure of acidity derived from ionization equilibria of an indicator behaving in the Brönsted-Lowry sense.

$$BH^+ = B + H^+ \quad \text{(Eq. 2)}$$

The acidity function (a unitless parameter) is defined by (Eq.3).

$$H_0 = pK_{BH} + \log (C_B/C_{BH}) \quad \text{(Eq. 3)}$$

It was determined using UV-visible spectroscopy with 4-chloro-2-nitroaniline as the acidity indicator since its pK_{BH} value (-0.89 at 19°C) falls within the range of interest. More details about the experimental procedure can be found in [14]. The pore solution pH of hardened materials was less acidic and could be measured using conventional pH-metry.

Mixing was performed using a laboratory mixer equipped with an anchor stirrer and rotating at 250 rpm for 5 min. Paste samples were then cast into airtight polypropylene boxes (20 mL of paste per box) and cured at 25 ± 1°C.

A first series of cement pastes was prepared by varying the Ca/P molar ratio from 0.96 to 1.92, while keeping constant the initial orthophosphoric acid concentration (9 $mol.L^{-1}$) in the mixing solution (Table 1). The l/s ratio, which is correlated to these two parameters, varied from 1 to 0.5 in these experiments. In a second series of experiments, the l/s ratio was fixed at 0.76 $mL.g^{-1}$ whereas the initial phosphoric acid concentration was increased from 7 to 16.6 $mol.L^{-1}$. As a consequence, the Ca/P molar ratio decreased from 1.63 to 1.78.

Table 1: Composition of the cement pastes (H_0 stands for the acidity function, the pastes are labelled $P_{X/Y/Z}$ where X, Y and Z stand for the Ca/P ratio, initial H_3PO_4 concentration and l/s ratio respectively).

	Paste reference	Ca/P (mol/mol)	$[H_3PO_4]_{tot}$ ($mol.L^{-1}$)	l/s (mL/g)	H_0	$V_{mixing\ solution}$ (mL)	$M_{wollastonite}$ (g)
Series 1	$P_{0.96/9/1}$	0.96	9	1.00	-1.85	50	50
	$P_{1.24/9/0.76}$	1.24	9	0.76	-1.85	38	50
	$P_{1.92/9/0.5}$	1.92	9	0.50	-1.85	25	50
Series 2	$P_{1.63/7/0.76}$	1.63	7	0.76	-1.28	38	50
	$P_{1.52/7.5/0.76}$	1.52	7.5	0.76	-1.40	38	50
	$P_{1.42/8/0.76}$	1.42	8	0.76	-1.56	38	50
	$P_{1.35/8.5/0.76}$	1.35	8.5	0.76	-1.70	38	50
	$P_{1.24/9.5/0.76}$	1.24	9.5	0.76	-1.99	38	50
	$P_{1.14/10/0.76}$	1.14	10	0.76	-2.13	38	50
	$P_{0.95/12/0.76}$	0.95	12	0.76	-2.89	38	50
	$P_{1.24/12/0.57}$	1.24	12	0.57	-2.89	28	50
	$P_{0.78/14.6/0.76}$	0.78	14.6	0.76	-3.61	38	50

2.2 Characterization techniques

A TAM AIR isothermal conduction microcalorimeter was used to investigate the hydration rate of cement pastes at 25°C. Experiments were performed on 2-g samples prepared outside of the calorimeter (see [14] for more details).

To stop cement hydration, pastes were first immersed into isopropanol, crushed by hand, filtrated and dried in an oven at 38°C for 24 h. Preliminary tests showed that this drying procedure did not change the phase assemblage as compared with drying at room temperature for several days.

The powder obtain after stopping the hydration was further ground by hand to a particle size below 100 µm and characterized by TGA and XRD, as described in a previous work [14]. Rietveld analysis was performed with the internal standard method, using silicon as the standard. Table 2 gives the ICDS number of the phases used for the refinement.

Table 2: ICDS files associated to crystalline phase

Crystalline phase	ICDS file
Brushite	72-0713
Monetite	70-0359
Wollastonite	84-0654
OCP	74-1301
Quartz	70-7344
Silicon	27-1402
CDHA	46-0905
MCPM	09-0347

The mechanical strength of 4×4×4 cm paste specimens was characterized after 28 d of curing at ambient temperature in a sealed bag to prevent desiccation. The compressive strength was measured following EN 196-1 European standard (loading rate: 2.4 $kN.s^{-1}$) with a mechanical compression testing machine (3R RP 40/400FC).

The pore solution of a 3 month-old hardened paste was extracted by compaction of about 140 g crushed sample using the device described by Cyr *et al*. [16] with a 3R RP-3000 QC mechanical press at a pressure up to 300 MPa. The pH of the recovered liquid was immediately measured with a pH electrode (Mettler Toledo InLab Expert Pt1000 pH 0–14 T 0–100 °C) calibrated using two pH buffers at 1.09 (25 °C) and 4.01 (25 °C).

143 *2.3 Thermodynamic modelling*

144 Experiments were supported by thermodynamic equilibrium modelling in order to predict
145 phase assemblages in the cement pastes as a function of their hydration degree. Thermodynamic
146 calculations were carried out using CHESS software which works by minimizing the free
147 energy of a pre-defined system [17]. The Chess database was enriched by adding new calcium
148 phosphate species relevant to the investigated system, as detailed in [14]. The activity
149 coefficients of the aqueous species were calculated using the B-dot model which is considered
150 to be reasonably accurate in predicting the activities of Na^+ and Cl^- ions to concentrations as
151 large as several $mol.kg^{-1}$, and of other species to ionic strengths up to 0.3 to 1 $mol.kg^{-1}$ [18].
152 Note that the ionic strength of the mixing solution was initially extremely high but rapidly
153 dropped below 0.75 $mol.L^{-1}$ when the products stated to precipitate.

154

155 **3. Results and discussion**

156

157 *3.1 Influence of the Ca/P and l/s ratios*

158 3.1.1. Hydration rate

159 Hydration of pastes $P_{0.96/9/1}$, $P_{1.27/9/0.76}$ and $P_{1.92/9/0.5}$, prepared with a 9 $mol.L^{-1}$ H_3PO_4 solution,
160 but having different Ca/P and l/s ratios, was monitored using isothermal microcalorimetry
161 (Figure 1). An increase in the Ca/P ratio, correlated with a decrease in the l/s ratio, accelerated
162 the hydration process: the duration of the period of low thermal activity decreased, as well as
163 the time at which the heat flow reached its maximum. The cumulative heat produced at 50 h
164 (normalized with respect to the mass of wollastonite) also diminished.

165

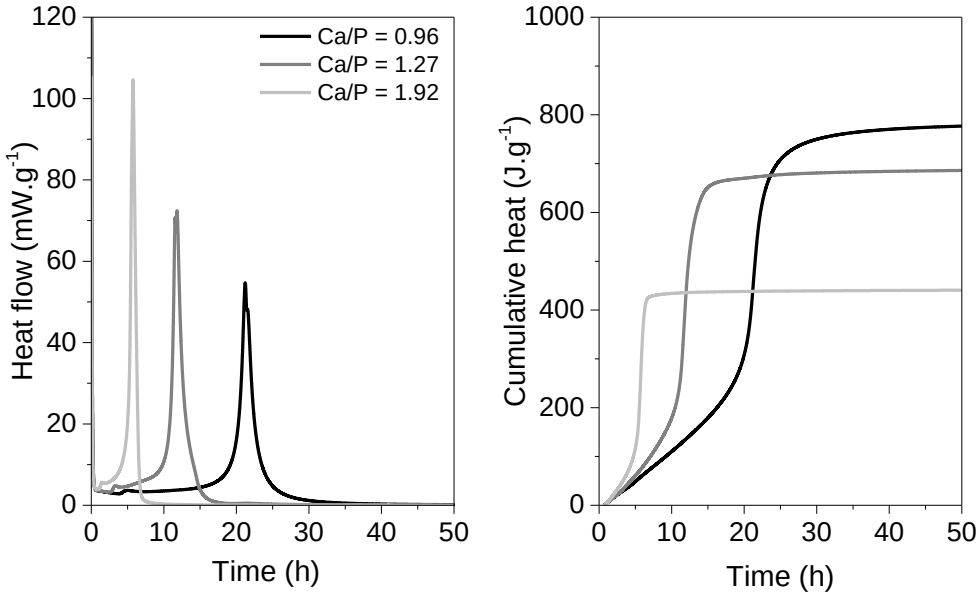

Figure 1: Heat flow (left) and cumulative heat (right) of pastes $P_{0.96/9/1}$, $P_{1.27/9/0.76}$ and $P_{1.92/9/0.5}$ (standardized with respect to the mass of wollastonite).

The heat measured in microcalorimetry results from the heat produced or absorbed by the reactions taking place during setting. Table 2, summarizing the enthalpies of the main possible reactions, shows that dissolution of wollastonite is strongly exothermic, whereas precipitation of hydroxyapatite (HA) or calcium-deficient hydroxyapatite (CDHA) is strongly endothermic. In comparison, precipitation of brushite, monocalcium phosphate monohydrate and monetite should have a much more limited effect on heat. The decrease in the cumulative heat observed in our study when the Ca/P ratio of the paste increased could thus result from a decrease in the fraction of dissolved wollastonite, but also from a change in the phase assemblage. Indeed, if precipitation of HA or CDHA is promoted at the expense of brushite at high Ca/P ratio, the heat released by the dissolution of wollastonite might be partly balanced by the heat absorbed by the precipitation of hydrates. To check these two hypotheses, it was necessary to determine the mineralogy of the hydrated cement pastes.

183 Table 2: Enthalpy of reactions that may occur during the hydration of wollastonite with an
184 orthophosphoric solution [19, 20].

Reaction	Balance equation	Enthalpy of reaction (kJ/mol)
Dissolution of wollastonite	$CaSiO_3 + 2\ H^+ + H_2O \rightarrow Ca^{2+} + Si(OH)_4$	-88.20
Precipitation of MCPM	$Ca^{2+} + 2\ H_3PO_4 + H_2O \rightarrow Ca(H_2PO_4)_2.H_2O + 2H^+$	-4.36
Precipitation of brushite	$Ca^{2+} + H_3PO_4 + 2H_2O \rightarrow CaHPO_4.2H_2O + 2H^+$	-0.77
Precipitation of monetite	$Ca^{2+} + H_3PO_4 \rightarrow CaHPO_4 + 2H^+$	16.77
Precipitation of OCP	$8\ Ca^{2+} + 6\ H_2PO_4^- + 5\ H_2O \rightarrow Ca_8(HPO_4)_2(PO_4)_4.5H2O + 10\ H^+$	Not available
Precipitation of HA	$5\ Ca^{2+} + 3\ H_2PO_4^- + H_2O \rightarrow Ca_5(PO_4)_3(OH) + 7\ H^+$	178.4
Precipitation of CDHA	$9\ Ca^{2+} + 6\ H_2PO_4^- + H_2O \rightarrow Ca_9(HPO_4)(PO_4)_5(OH) + 12\ H^+$	228.9
Conversion MCPM → Monetite	$Ca(H_2PO_4)_2.H_2O \rightarrow CaHPO_4 + H_3PO_4 + H_2O$	21.43
Conversion MCPM → Brushite	$Ca(H_2PO_4)_2.H_2O + H_2O \rightarrow CaHPO_4.2H_2O + H_3PO_4$	3.59

185

186 3.1.2. Phase assemblage

187 The X-ray diffraction patterns of the 7-d old cement pastes are compared in Figure 2A.
188 Wollastonite, brushite, quartz and monetite were evidenced whatever the sample. In addition,
189 the paste with the highest Ca/P ratio contained small amounts of hydroxyapatite (HA or CDHA)
190 and octacalcium phosphate (OCP). The Rietveld quantification (Figure 2B) showed the
191 presence of an amorphous phase which was likely amorphous silica. Its amount was indeed in
192 good agreement with that calculated for silica using equation (Eq. 5) and the amount of
193 consumed wollastonite (Figure 3).

194 $CaSiO_3 + 2H^+ + (x\text{-}1)\ H_2O \rightarrow Ca^{2+} + SiO_2.xH_2O$ (Eq. 5)

195

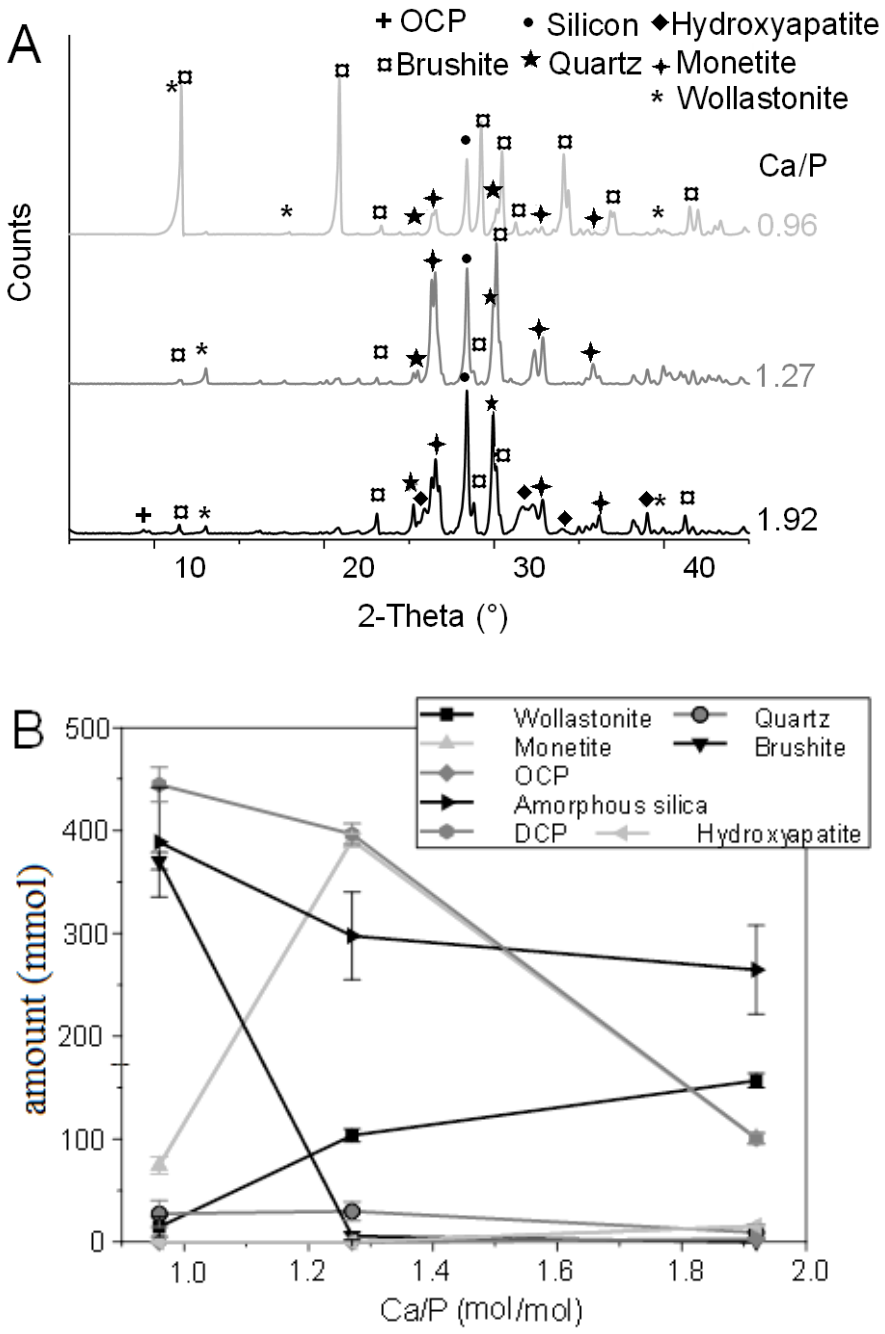

Figure 2: X-ray diffraction patterns of pastes $P_{0.96/9/1}$, $P_{1.27/9/0.76}$ and $P_{1.92/9/0.5}$ after 7 d of curing (A) and phase evolution as a function of the Ca/P molar ratio at 7 d (B) (OCP: octacalcium phosphate, DCP: dicalcium phosphate (monetite + brushite)).

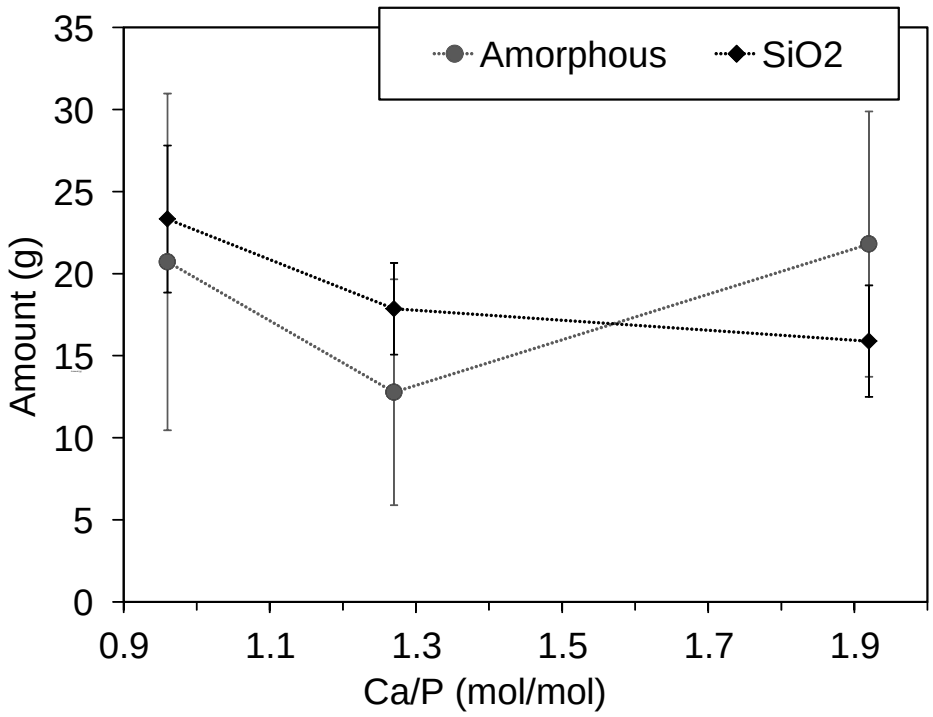

Figure 3: Comparison of the amounts of silica calculated from consumed wollastonite and of total amorphous phase in pastes $P_{0.96/9/1}$, $P_{1.27/9/0.76}$ and $P_{1.92/9/0.5}$ after 7 d of curing.

The fraction of wollastonite consumed at 7 d was calculated from the Rietveld results: 97 ± 8 % for paste $P_{0.96/9/1}$, 76 ± 6 % for paste $P_{1.27/9/0.76}$ and 64 ± 7 % for paste $P_{1.92/9/0.5}$. Increasing the Ca/P ratio (and decreasing the l/s ratio) thus limited the consumption degree of wollastonite at 7 d. Several reasons can be postulated:

- a lack of water at low l/s ratio;
- a faster decrease in the acidity of the interstitial solution, which slowed down the dissolution of wollastonite [21];
- rapid precipitation of dense layers of hydrates around the wollastonite particles, which made it more difficult for water molecules to react with this mineral.

Increasing the Ca/P ratio also modified the mineralogy: OCP and hydroxyapatite were observed at high Ca/P ratio whereas the amount of dicalcium phosphate strongly decreased. Therefore, the smaller cumulative heat reported at high Ca/P ratio in the previous section

resulted both from a decrease in the degree of hydration (less wollastonite was consumed) and from the precipitation of hydroxyapatite, an endothermic reaction partly compensating for the exothermic dissolution of wollastonite. The type dicalcium phosphate formed also depended on the Ca/P ratio: brushite ($CaHPO_4.2H_2O$) was the main phase at Ca/P 0.96, whereas monetite ($CaHPO_4$) predominated at higher ratios. This result is closely related to the evolution of the maximum heat flow observed by microcalorimetry. The higher the heat flow, the higher the self-heating of the material during hydration, which favours the precipitation of monetite at the expense of brushite [5]. In fact the thermal evolution of the paste with time has been recorded: a significant temperature rise was observed a few hours after mixing (the temperature of the sample reached 67.7°C at 16 h), which promoted the precipitation of monetite.

3.1.3. Thermodynamic modelling

The reaction of wollastonite with a H_3PO_4 solution was simulated using Chess software at different Ca/P molar ratios. The input data were the amounts of liquid and solid phases and the initial H_3PO_4 concentration used to prepare pastes $P_{0.96/9/1}$, $P_{1.27/9/0.76}$ and $P_{1.92/9/0.5}$. Table 3 shows the calculated phase assemblages for degrees of wollastonite consumption corresponding to those measured experimentally after 7 d of hydration. Two differences were noticed as compared with the experiments:

- the calculations always predicted the formation of monetite instead of brushite since monetite is the most stable phase at 25°C from a thermodynamic point of view [19],
- monocalcium phosphate monohydrate (MCPM) was expected to form at the lowest Ca/P ratio of 0.96. The calculated amount was however very small (2.6%), which could explain why this mineral was not evidenced by X-ray diffraction.

The calculated amount of monetite decreased when the Ca/P ratio increased, which was in good agreement with the experimental results. The simulation also predicted the formation of

hydroxyapatite at a Ca/P ratio of 1.92, which again was consistent with the experimental observations.

Table 3: Thermodynamic modelling results at 25°C

Ca/P	Progress of wollastonite dissolution (%)	MCPM (mmol)	Monetite (mmol)	HA (mmol)	Silica (mmol)
0.96	97	8.5	398	0	418
1.24	76	0	322	0	308
1.92	64	0	117	36	275

3.2 Effect of phosphoric acid concentration and acidity

3.2.1. Hydration rate

Figure 4 shows the heat flux and cumulative heat produced by the second series of cement pastes, prepared at constant l/s ratio, but with a variable H_3PO_4 concentration in the mixing solution, and thus a variable Ca/P ratio. The initial H_3PO_4 concentration strongly influenced the rate of hydration. Its increase within the range 7 - 10 mol.L^{-1} increased the duration of the low thermal activity period and the cumulative heat produced at the end of the experiment, but decreased the maximal heat flow.

As previously, two processes could contribute to increase the cumulative heat flow: a higher dissolution degree of wollastonite, and a decrease in the progress of endothermic reactions (mainly hydroxyapatite precipitation). For H_3PO_4 concentrations above 12 mol.L^{-1}, no heat flow peak was observed, even after 7 days, and the cumulative heat remained of small magnitude. The pastes prepared with these solutions exhibited a stiffening but no setting was observed after 3 months.

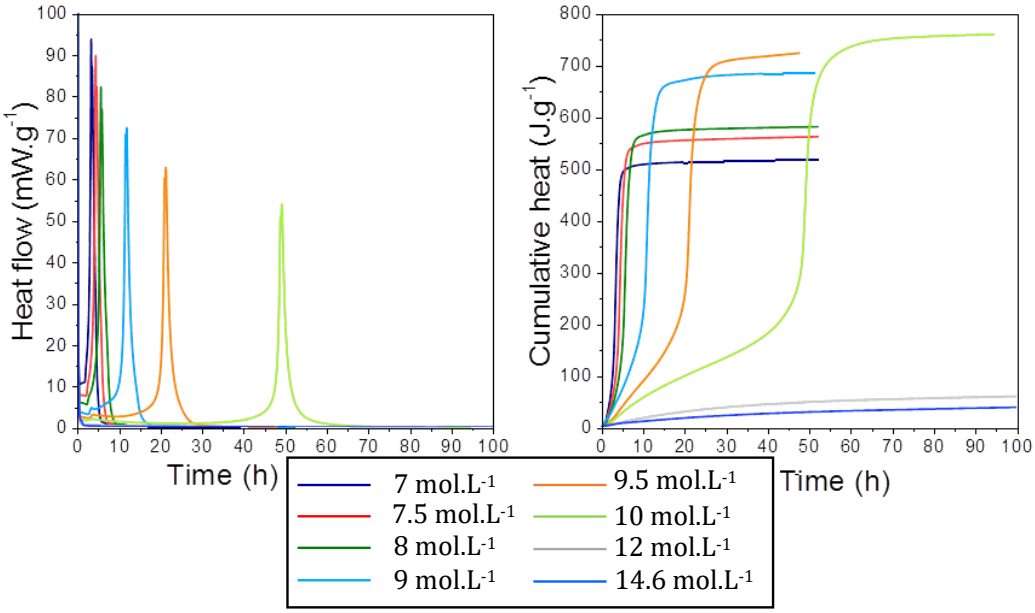

Figure 4: Heat flow (left) and cumulative heat (right) of cement pastes $P_{1.63/7/0.76}$, $P_{1.52/7.5/0.76}$, $P_{1.42/8/0.76}$, $P_{1.35/8.5/0.76}$, $P_{1.24/9/0.76}$, $P_{1.20/9.5/0.76}$, $P_{1.14/10/0.76}$, $P_{0.95/12/0.76}$ and $P_{0.78/14.6/0.76}$ (standardization with respect to the mass of wollastonite).

Raising the H_3PO_4 concentration not only decreased the Ca/P molar ratio of the cement paste, but also increased the acidity of the mixing solution. The acidity function value H_0 was measured for each investigated H_3PO_4 concentration (Figure 5-A). The results were consistent with those of previous studies [26, 27]. The maximal heat flow, the corresponding ageing time ($t(FQ_{max})$) and the maximal cumulative heat were then plotted as a function of the acidity function of the mixing solution (Figure 5-B, C, D). The maximal heat flow and cumulative heat varied linearly with the acidity function. The smaller the acidity function (i.e. the higher the acidity), the smaller the maximal heat flow, but the higher the cumulative heat released at the end of the experiment. As for time $t(FQ_{max})$, it decreased exponentially when the acidity function increased.

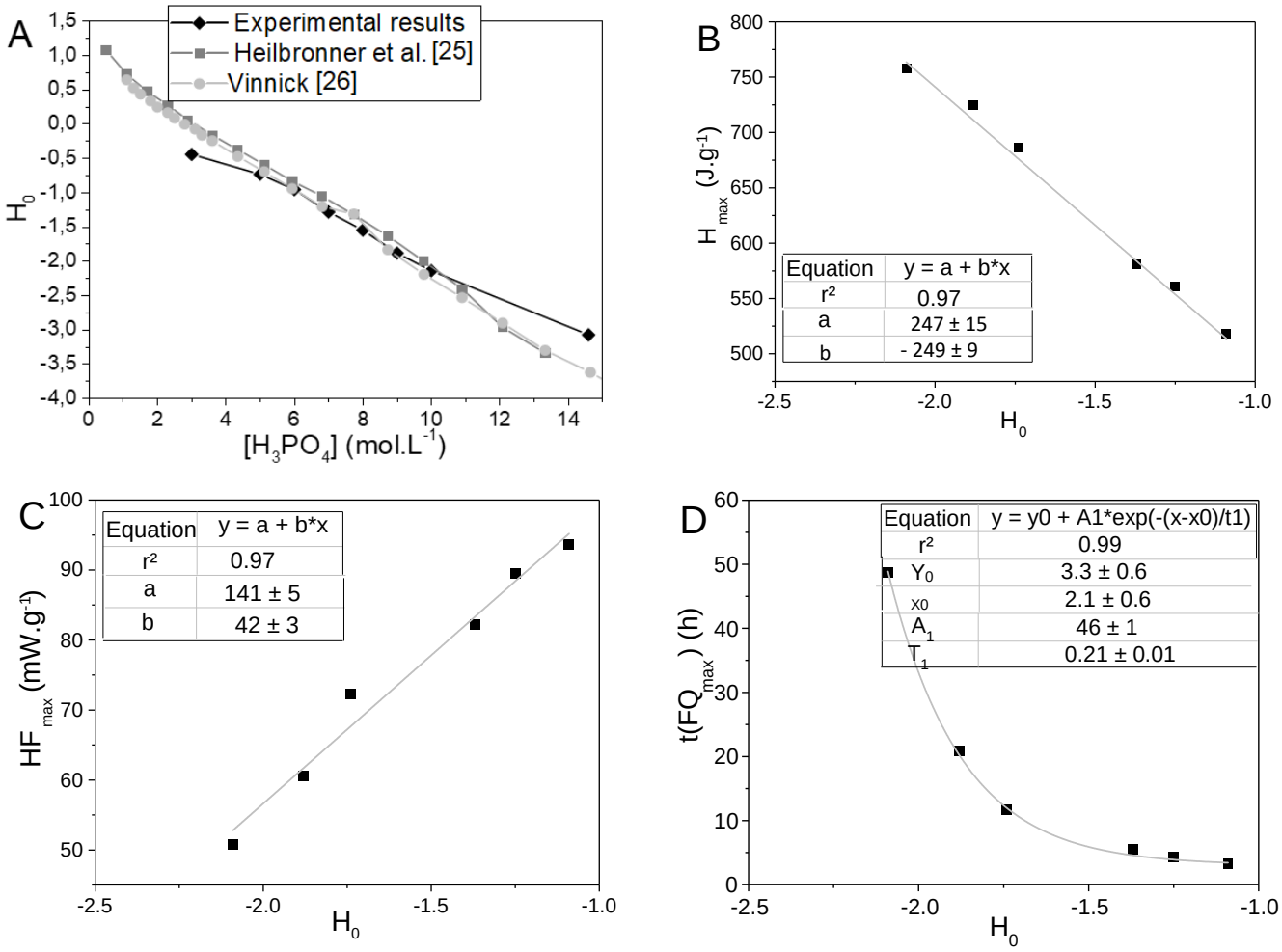

279 Figure 5: Evolution of the acidity function (H_0) with the phosphoric acid concentration (A),
280 Evolution of the maximal cumulative heat (B), maximal heat flow (C) and corresponding ageing
281 time (D) as a function of the acidity function.

282

283 The absence of any setting or heat flow peak for the pastes prepared with a H_3PO_4 solution
284 at a concentration ≥ 12 mol.L^{-1} raised several questions. Did wollastonite react under these
285 conditions? What was the limiting factor, a lack of water, a too low Ca/P ratio (below 1) to
286 make it possible to precipitate brushite or monetite (Ca/P = 1), a too strong acidity as compared
287 with the stability domain of brushite or monetite (c.a. 2 ≤ pH ≤ 6 [22]) ? To investigate the
288 influence of the Ca/P ratio, a supplementary paste sample was prepared with a 12 mol.L^{-1} H_3PO_4
289 solution, but with a smaller l/s ratio (0.57 mL.g^{-1} instead of 0.76 mL.g^{-1}) in order to get a Ca/P
290 ratio of 1.24, as for paste $P_{1.24/9/0.76}$ prepared with a 9 mol.L^{-1} H_3PO_4 solution. Hydration was

monitored by microcalorimetry: no heat flow peak could be detected despite the higher Ca/P ratio. This rules out the hypothesis of a limitation due to a deficit in calcium. Mineralogical characterizations were thus required to get a better understanding of the cement reactivity.

3.2.2. Phase assemblage

The phase evolution of paste $P_{1.20/9.5/0.76}$ with ongoing hydration was first investigated by X-ray diffraction (Figure 6). Wollastonite was almost fully consumed after 48 h. MCPM precipitated transiently at 10 h, and dissolved afterwards. Monetite was the main product, but small amounts of brushite were evidenced at 7 days. Brushite formed afterwards, when the sample cooled back to room temperature.

Comparing the mineralogical evolution and calorimetric data (Figure 6) shows that the heat flow peak seemed to occur simultaneously with the conversion of MCPM into monetite. Note that this reaction, which is slightly endothermic (Table 3) could not explain by itself the heat release, but it was associated with an accelerated dissolution of wollastonite, which is a strongly exothermic process, and its precipitation into monetite.

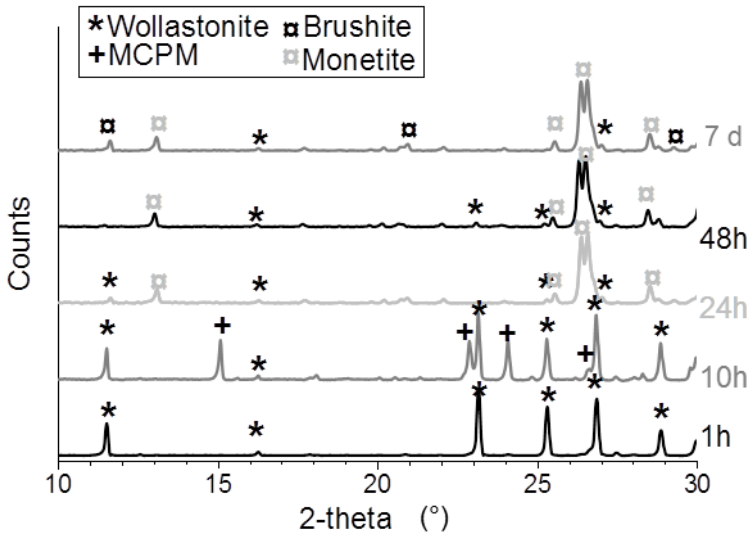

Figure 6: X-ray diffraction patterns of paste $P_{1.20/9.5/0.76}$ aged from 1 h to 7 d

The X-ray diffraction patterns of the 7 d-old samples prepared with H_3PO_4 solutions of increasing concentrations (from 7 to 14.6 mol.L^{-1}) were refined using Rietveld analysis. Figure 7 plots the evolution of the amounts of crystalline and amorphous phases as a function of the initial H_3PO_4 concentration. As previously, the amount of amorphous phase fitted rather well with that calculated for silica using (Eq. 2) and the amount of residual wollastonite (Figure 8). This latter exihibited a non-monotonous evolution: it started to decrease when the H_3PO_4 concentration was raised from 7 to 9.5 mol.L^{-1}, and increased at higher concentrations. The amount of precipitated calcium diphosphate (monetite + brushite) showed opposite variations.

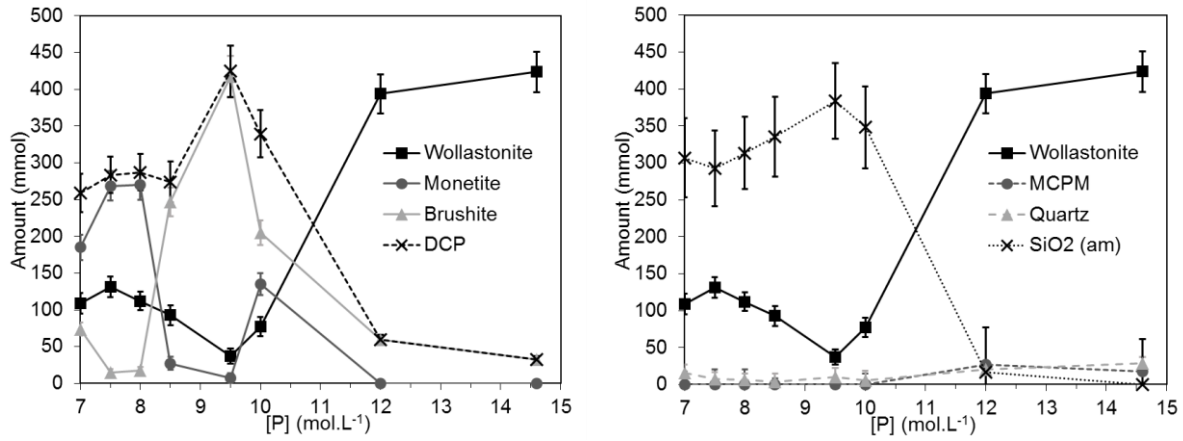

Figure 7: Phase evolution as a function of the Ca/P molar ratio of pastes $P_{1.63/7/0.76}$, $P_{1.52/7.5/0.76}$, $P_{1.42/8/0.76}$, $P_{1.35/8.5/0.76}$, $P_{1.24/9/0.76}$, $P_{1.20/9.5/0.76}$, $P_{1.14/10/0.76}$, $P_{0.95/12/0.76}$ and $P_{0.78/14.6/0.76}$ after 7 d of curing (DCP: dicalcium phosphate (monetite + brushite)).

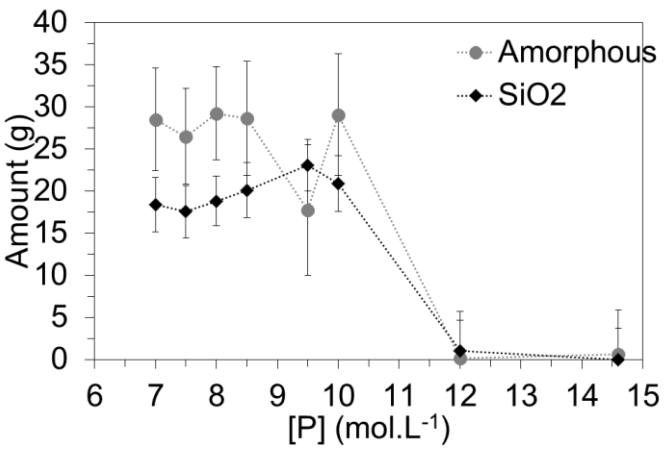

Figure 8: Comparison of the amount of calculated silica from reacted wollastonite and total amorphous phase in $P_{1.63/7/0.76}$, $P_{1.52/7.5/0.76}$, $P_{1.42/8/0.76}$, $P_{1.35/8.5/0.76}$, $P_{1.24/9/0.76}$, $P_{1.20/9.5/0.76}$, $P_{1.14/10/0.76}$, $P_{0.95/12/0.76}$ and $P_{0.78/14.6/0.76}$ after 7 d of curing

At elevated H_3PO_4 concentrations (12 and 14.6 mol.L^{-1}), only a small fraction of wollastonite had reacted at 7 d (9% and 2% respectively) (Table 4) to form MCPM and brushite, which could explain the absence of setting. MCPM was still observed after a few months of curing under sealed bag (results not shown here). The persistence of MCPM could result from several factors: a lack of water which blocked the reactions, or a too low pH for dicalcium phosphate to precipitate. To check the first assumption, 7 d-old $P_{0.95/12/0.76}$ and $P_{0.78/14.6/0.76}$ samples were characterized using thermogravimetry analysis in order to determine the amount of water bound in the solid phase. This latter represented 45% (paste $P_{0.95/12/0.76}$) or 71 % ($P_{0.78/14.6/0.76}$) of the total water (Table 5). There was thus some residual free water in these samples at 7 d, making the assumption of a lack of water rather unlikely. The interstitial solution of paste $P_{0.95/12/0.76}$ and $P_{0.78/14.4/0.76}$ was extracted using pressure after 3 months of curing. Its pH was found to be close to 1, i.e. within the stability domain of MCPM [22].

341 Table 4: Fraction of wollastonite depleted at 7 d as a function of the initial H_3PO_4

342 concentration.

$[H_3PO_4]$ (mol.L^{-1})	Depleted wollastonite (%)
7.0	75
7.5	69
8.0	74
9.0	76
9.5	91
10.0	82
12.0	9
14.6	2

343

344 Table 5: Total and bound water contents in 7 d-old pastes $P_{0.95/12/0.76}$ and $P_{0.78/14.6/0.76}$.

H_3PO_4 concentration	Initial water content (%)	Water content in the solid phase at 7 days (%)
12.0 mol.L^{-1}	13.1	4.4
14.6 mol.L^{-1}	8.3	3.3

345

346 The maximal cumulative heat measured by isothermal microcalorimetry was strongly
347 correlated with the consumption degree of wollastonite inferred from Rietveld refinements
348 (Figure 9). Dissolution of wollastonite was thus the main process governing the heat production
349 in the second series of cement pastes: the higher the cumulative heat, the higher the extent of
350 dissolution of wollastonite.

351

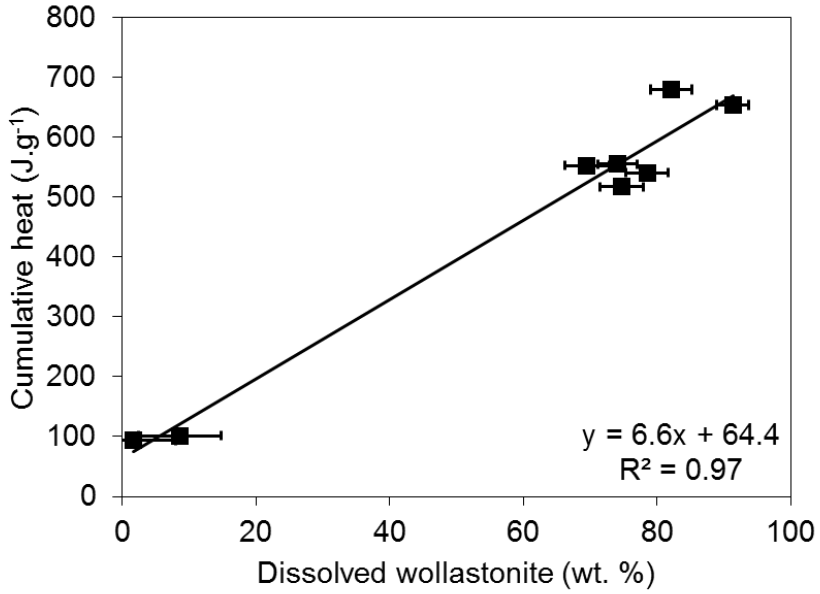

352

353 Figure 9: Cumulative heat as a function of the fraction of wollastonite depleted at 7 d.

354

355 3.2.3. Thermodynamic modelling

356 The mineralogical evolution of paste $P_{1.20/9.5/0.76}$ with ongoing hydration was simulated using
357 CHESS software (Figure 10). Thermodynamic modelling well predicted the transient
358 precipitation of MCPM before that of monetite, which occurred when the pore solution pH
359 reached a value close to 2.5.

360

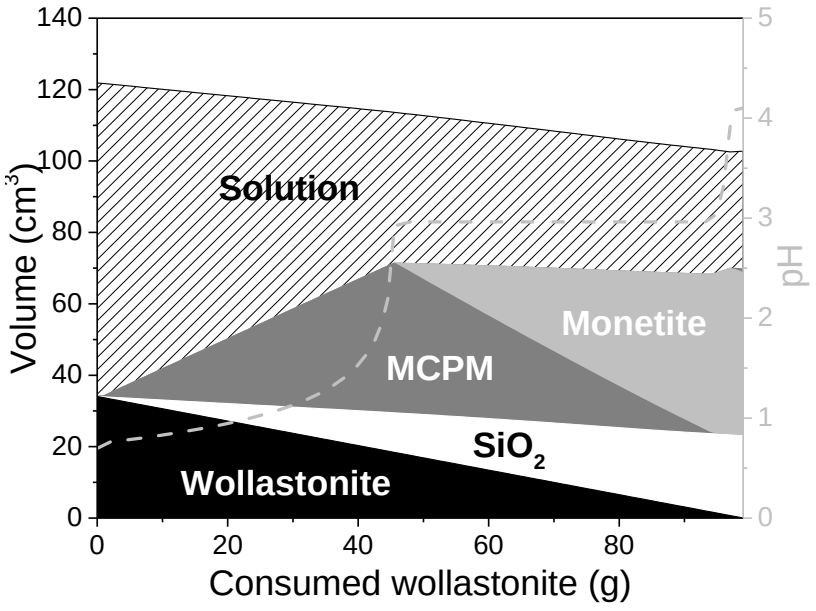

361

362 Figure 10: Thermodynamic simulation of the hydration of paste $P_{1.20/9.5/0.76}$ (100 g of
363 wollastonite + 76 mL of a 9.5 mol.L^{-1} H_3PO_4 solution)

364

365 Thermodynamic calculations were also carried out to determine the phase assemblage in
366 pastes $P_{1.63/7/0.76}$, $P_{1.42/8/0.76}$, $P_{1.20/9.5/0.76}$, $P_{1.14/10/0.76}$, $P_{0.95/12/0.76}$ and $P_{0.78/14.6/0.76}$ at the same degree
367 of wollastonite dissolution as in the 7-d old samples. Experimental and calculated results are
368 compared in Table 6. As previously, thermodynamics predicted the formation of monetite,
369 which is more stable than brushite at 25°C [23]. Hydroxyapatite was also expected to form in
370 the pastes prepared with the least acidic solution. This phase was not detected experimentally,
371 possibly because it was present in rather small amounts (close to the detection limit of X-ray
372 diffraction), or because the precipitation of hydroxyapatite is often preceded by that of an
373 amorphous calcium phosphate mineral [24, 25] which could not be evidenced with the
374 techniques used in this study. In contrast, the formation of MCPM, experimentally observed for
375 the more concentrated H_3PO_4 solutions and smallest degrees of hydration, was well depicted
376 by the model.

377

378 Table 6: Experimental and calculated phase assemblages of pastes $P_{1.63/7/0.76}$, $P_{1.42/8/0.76}$,
379 $P_{1.20/9.5/0.76}$, $P_{1.14/10/0.76}$, $P_{0.95/12/0.76}$ and $P_{0.78/14.6/0.76}$ after 7 d of hydration.

380

[H_3PO_4]	Consumed wollastonite	MCPM (mmol)		Dicalcium phosphate (mmol)		Hydroxyapatite (mmol)		Silica (mmol)	
mol.L^{-1}	%	Simulation	Experiment	Simulation	Experiment	Simulation	Experiment	Simulation	Experiment
7.0	75	0	0	332	259	66	0	304	307
8.0	74	0	0	544	287	22	0	299	313
9.5	91	0	0	559	425	52	0	362	384
10.0	82	12	0	676	340	0	0	328	348
12.0	9	64	4	0	60	0	0	33	17
14.6	2	4	2	0	32	0	0	3	0

381

Finally, the model was used to calculate the amount of wollastonite needed to be consumed before the destabilization of MCPM. This amount increased with the initial H_3PO_4 concentration (Figure 11), which can explain why the heat flow peak, associated with the conversion of MCPM into monetite, was experimentally delayed when the phosphoric acid concentration increased.

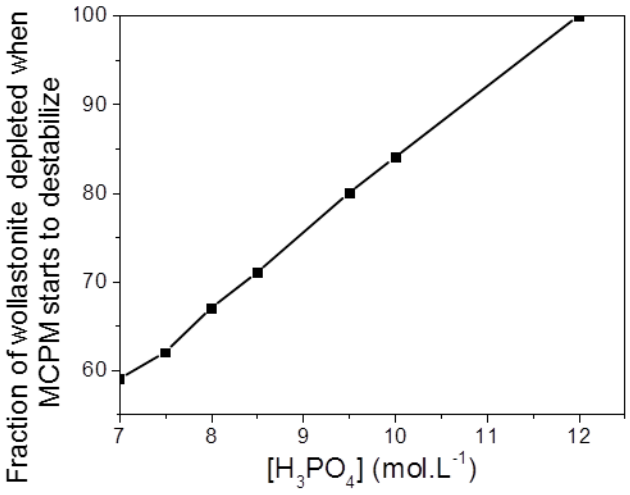

Figure 11: Fraction of wollastonite needed to be dissolved to destabilize MCPM.

3.2.4. Mechanical strength

After 28 d of curing at room temperature in sealed bag, the paste samples prepared with the the different H_3PO_4 concentrations were still very friable. Several visual aspects indicated a poor mechanical behaviour such as cracks at the surface of samples and swelling. This was confirmed by measuring their compressive strength: all the results were below 1 MPa, which means that the sole presence of phosphoric acid in the mixing solution did not make it possible to get a hardened paste with good mechanical properties (tests were repeated several time to make sure this was not an experimental bias). This poor mechanical behaviour likely resulted from a very porous microstructure. SEM observation of a 2 d-old fracture (the hydration did not progress a lot afterwards) of paste $P_{1.24/9/0.76}$ showed the presence of platelet crystals, assigned to monetite, and agglomerated into nodules, with large voids between the nodules

(Figure 12). Metallic cations, present in the mixing solution of commercial cements, thus play a key role in the consolidation process of the material.

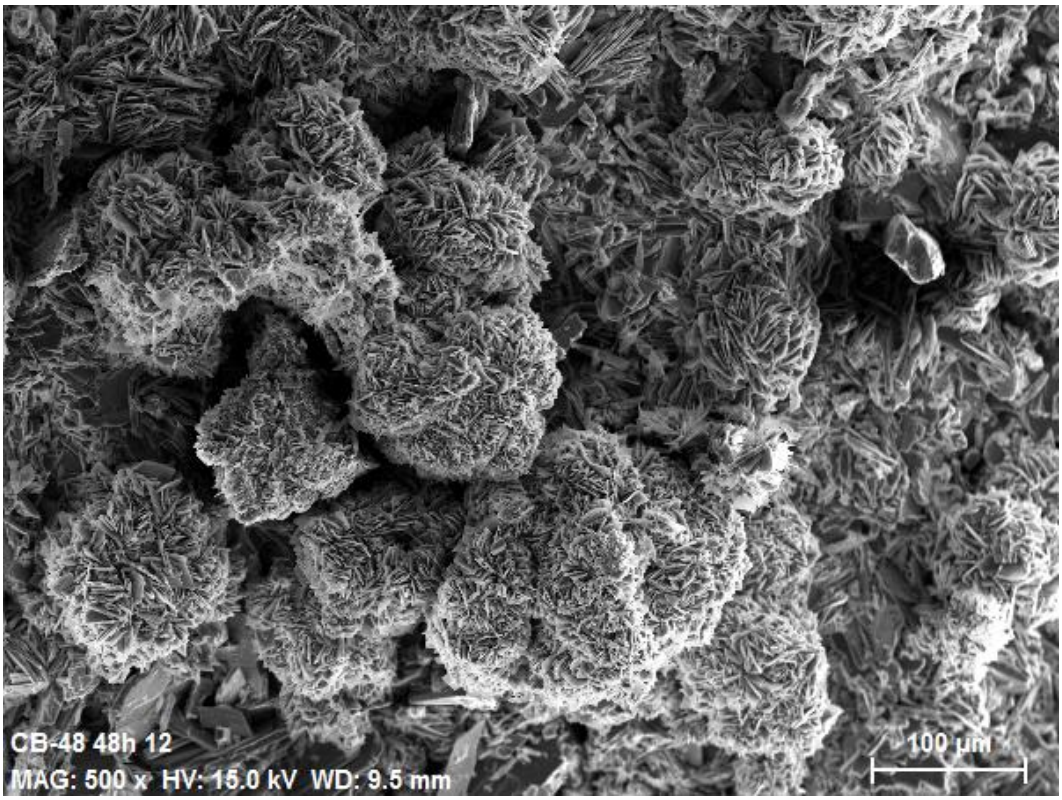

Figure 12: SEM observation of a fracture of paste sample PXXX after 2 d of hydration.

3. Conclusion

Brushite cements can be prepared by mixing wollastonite with a phosphoric acid solution usually containing boric acid or sodium borate (some retarders) and metallic cations (Zn^{2+}, Al^{3+}, Mg^{2+}...). However, the influence of the mixing solution composition on the setting and hardening process still needs to be clarified. In this work, dedicated to simplified systems comprising only wollastonite and phosphoric acid solutions of variable concentrations, three parameters were more particularly investigated: the Ca/P molar ratio, the H_3PO_4 initial

concentration, and the l/s weight ratio. Note that these parameters are correlated: setting the Ca/P ratio and H_3PO_4 concentration defines for instance the l/s ratio.

At constant H_3PO_4 concentration, the Ca/P ratio, correlated to the l/s ratio, not only influenced the hydration rate, but also the nature of the products formed during hydration. The higher the Ca/P ratio (and the lower the l/s ratio), the faster the start of hydration, but the smaller the fraction of wollastonite reacting, and the smaller the amount of dicalcium phosphate (anhydrous or dihydrate) formed. Moreover, the precipitation of more basic calcium orthophosphates (octacalcium phosphate and hydroxyapatite) occurred at high Ca/P ratio (1.92). The type of dicalcium phosphate precipitating depended on the thermal history of the sample: a high self-heating resulted in the formation of monetite ($CaHPO_4$) instead of brushite ($CaHPO_4.2H_2O$).

At constant l/s ratio (0.76 $mL.g^{-1}$), increasing the H_3PO_4 concentration in the range 7 to 10 $mol.L^{-1}$ (and thus decreasing the Ca/P ratio from 1.52 to 1.14) delayed cement hydration. After the transient precipitation of monocalcium phosphate monohydrate ($Ca(H_2PO_4)_2.H_2O$), both brushite ($CaHPO_4.2H_2O$) and monetite ($CaHPO_4.2H_2O$) formed. Their total amount, as well as the fraction of depleted wollastonite, reached a maximum for a 9.5 $mol.L^{-1}$ H_3PO_4 concentration. Setting the H_3PO_4 concentration within the range 9 - 10 $mol.L^{-1}$ could thus be recommended: hydration was not too fast and a large amount of dicalcium phosphate was formed under these conditions. At more elevated H_3PO_4 concentrations ($\geq$ 12 $mol.L^{-1}$), setting was inhibited, and the heat production remained very low, indicating limited dissolution of wollastonite. Monocalcium phosphate monohydrate was the only product formed. Its conversion into dicalcium phosphate did not occur because of the too strong acidity of interstitial solution (pH $\approx$ 1).

The different phase assemblages obtained experimentally as a function of the H_3PO_4 concentration, Ca/P and l/s ratios were rather well reproduced by thermodynamic modelling.

Finally, it should be outlined that the consolidation of the pastes after setting remained rather limited: their compressive strength did not exceed 1 MPa after 28 d of curing under sealed bag at room temperature. Metallic cations and borax or boric acid, present in the mixing solution of commercial cements, must thus play a key role in the hardening process of the material. Future work should thus investigate their influence into more details.

Acknowledgements

Acknowledgements are due to Pascal Antonucci for his help in the laboratory.

References

[1] A.S. Wagh, Chemically bonded phosphate ceramics: twenty first century materials with diverse applications, 2nd ed, Elsevier Science Ltd, Oxford, 2016, 422 p.

[2] A. D. Wilson, J. W. Nichloson, Acid-base cements: Their biomedical and insdustrial applications, Cambridge University Press, Cambridge, 1993, 398 p.

[3] C. E. Semler, Lime silico phosphate ceramics, The United States department of Transportation, Washington DC, USA, (1974) p 6 3,804,661.

[4] C.E Semler, A quick-setting wollastonite phosphate cement, Ceram. Bull. 55 (1976) 983-988.

[5] M. Alshaaer, H. Cuypers, H. Rahier and J. Wastiels, Production of monetite-based Inorganic Phosphate Cement (M-IPC) using hydrothermal post curing (HTPC), Cem. Concr. Res. 41 (2011) 30-37.

[6] X. Wu, J. Gu, Inorganic resins composition, their preparation and use thereof, Vrije Universiteit Brussel, Belgium, EP 0 861 216 B1 (2000) 15.

[7] H. A. Colorado, C. Hiel, T. Hahn, J. M. Yang, Wollastonite based chemically bonded phosphate ceramics composites, in: J. Cuppoletti (Ed.) Metal, Ceramic and Polymeric Composites for Various Uses, InTech, Croatia, 2011, pp 265-282.

[8] H. A. Colorado, J. Pleitt, C. Hiel, J. M. Yang, H. T. Hahn, C. H. Castano, Wollastonite based-Chemically Bonded Phosphate Ceramics with lead oxide contents under gamma irradiation, J. Nucl. Mater. 425 (2012) 197-204.

[9] P. Laniesse, C. Cau Dit Coumes, P. Antonucci, G. Le Saout, A. Mesbah, P. Gaveau, Investigation of the hydration process of a wollastonite-based brushite cement for waste conditioning, Proc. 37th Cem. Concr. Sci. Conf., London, UK, September 11-12, 2017.

[10] P. Laniesse, C. Cau Dit Coumes, Y. Barre, A. Mesbah, G. Le Saout, P. Gaveau, G. Silly, Wollastonite-based brushite cement – Hydration process and strontium retention, Proc. NUWCEM 2018 (International symposium on cement-based materials for nuclear wastes), Avignon, France, October 24-26, 2018.

[11] G. Mosselmans, M. Biesemans, R. Willem, J. Wastiels, M. Leermakers, H. Rahier, S. Brughmans, B. Van Mele, Thermal hardening and structure of a phosphorus containing cementitious model material, J. Therm. Anal. Calorim. 88 (2007) 723-729.

[12] M. Alshaaer, H. Cuypers, G. Mosselmans, H. Rahier, J. Wastiels, Evaluation of a low temperature hardening Inorganic Phosphate Cement for high-temperature applications, Cem. Concr. Res. 41 (2011) 38-45.

[13] H. A. Colorado, Z. Wang, J.-M. Yang, Inorganic phosphate cement fabricated with wollastonite, barium titanate, and phosphoric acid, Cem. Concr. Compos. 62 (2015) 13-21.

[14] P. Laniesse, C. Cau Dit Coumes, A. Poulesquen, A. Bourchy, A. Mesbah, G. Le Saout, P. Gaveau, Setting and hardening process of a wollastonite-based brushite cement, Cem. Concr. Res. 106 (2018) 65-76

[15] L. P. Hammett, The theory of acidity, J. Am. Chem. Soc. 50 (1928) 2666-2673.

[16] M. Cyr, A. Daidie, Optimization of a high-pressure pore water extraction device, Rev. Sci. Instrum. 78 023906 (2007) 1-8

[17] J. Van der Lee, Thermodynamic and mathematical concepts of CHESS, Technical report LHM/RD/98/39, CIG, Ecole des Mines de Paris, Fontainebleau, France, 1998.

[18] H. C. Helgeson, Thermodynamics of complex formation in aqueous solution at elevated temperatures and pressures, Am. J. Sci. (1967) 729-804.

[19] H. C. Helgeson, J. M. Delany, H. W. Nesbitt and D. K. Bird, Summary and critique of the thermodynamic properties of rock forming minerals, Amer. J. Sci. 278A (1978) 1-229.

[20] P. Vieillard, Y. Tardy, Thermochemical Properties of Phosphates, in: J.O. Nriagu, P.B. More (Eds.), Phosphate Minerals, Springer Verlag, Berlin, 1984, pp 171-198.

[21] J. Schott, O. S. Pokrovsky, O. Spalla, F. Devreux, A. Gloter, J. A. Mielczarski, Formation, growth and transformation of leached layers during silicate minerals dissolution: the example of wollastonite, Geochim. Cosmochim. Acta 98 (2012) 259–281.

[22] V. Dorozhkin, Calcium orthophosphate cements and concretes, Materials 2 (2009) 221-291.

[23] C. Janot, B. Ilschner, Biocéramiques et biociments résorbables pour le comblement osseux, in: Traité des matériaux : Matériaux émergents, Presses polytechniques et universitaires Romandes, Lausanne, 2001, 436 p.

[24] E.D. Eanes, I.H. Gillessen, A.S. Posner, Intermediate states in the precipitation of hydroxyapatite, Nature 208 (1965) 365–367.

[25] J.C. Elliott, General chemistry of the calcium orthophosphates, in: J.C. Elliott (Ed.), Structure and Chemistry of the Apatites and Other Calcium Orthophosphates, Elsevier, Amsterdam, 1994, pp. 1–62.

[26] E. Heibronner, S. Weber, Die Hammett'sche Säurefunktion des Systems Phosphorsäure / Wasser, Helvet. Chim. Act. 32 (1949) 1513-1517

[27] Vinnick, M.I., Acidity functions of aqueous solutions of strong acids, Russian Chemical Review, 35 (1966) 802-817.